COMMUNICATION www.rsc.org/chemcomm | ChemComm

Assembly between gold-thiolate nanoparticles and the organometallic cluster $[Fe(\eta^5\text{-}C_5H_5)(\mu_3\text{-}CO)]_4$ toward redox sensing of oxo-anions†

Jaime Ruiz Aranzaes, Colette Belin and Didier Astruc*

Received (in Cambridge, UK) 5th June 2007, Accepted 6th July 2007
First published as an Advance Article on the web 25th July 2007
DOI: 10.1039/b708466h

Covalent assembly between gold-thiolate nanoparticles (AuNPs) and the cluster $[Fe(\eta^5\text{-}C_5H_5)(\mu_3\text{-}CO)]_4$, 1, can be achieved either by direct Brust–Schriffin-type synthesis using a mixture of undecanethiol and a thiol functionalized with 1, or by substitution of undecanethiolate ligands in AuNPs by thiolate ligands functionalized with 1; cyclic voltammetry of these AuNPs functionalized with 1 allows us to recognize and titrate the oxo-anions $H_2PO_4^-$ and ATP^{2-}.

Anion sensing is a modern topic of high interest given the key roles of anions in biology and the environment. It has been investigated *inter alia* using redox sensors[1] attached to endo[1,2]- or exo-receptors[3,4] and the redox system that is chosen for anion sensing most often involves ferrocene. The latter is reliable and convenient,[5,6] and ferrocenyl-terminated dendrimers[7] are an example of such an application.[8] The long-known organometallic cluster $[Fe(\eta^5\text{-}C_5H_5)(\mu_3\text{-}CO)]_4$, **1**, is another example of a robust redox system (Fe_4/Fe_4^+), the oxidation of the neutral cluster to the cationic one being fully reversible and located at as mild a potential as that of ferrocene.[9] This cluster is larger than ferrocene, however, and presents several potential sites for supramolecular interactions by hydrogen bonding, such as the four carbonyl ligands. Indeed, attempts to decorate dendrimers with these clusters showed promising results.[10] Gold nanoparticles (AuNPs)[11,12] have been shown to be particularly useful for redox sensing, because they can be readily assembled with a large number of branch termini, such as ferrocenyl.[13]

The cluster **1** bearing an amido substituent does not recognize oxo-anions, and we will show here that AuNPs serve as templates to assemble nanostructures whose many tethers bearing the amido-cluster derived from **1** recognize $H_2PO_4^-$ and ATP^{2-}. The electrochemical response in such assemblies distinguishes between the redox centers that are connected to the guest species by supramolecular interactions and those that are not.[13]

Stable AuNPs functionalized with the thiolate ligands derivatized with the cluster **1** were synthesized using two strategies as follows. First, undecanethiolate substitution by the thiolate anion of the air-sensitive cluster-thiol $[Fe_4(\mu_3\text{-}CO)_4(\eta^5\text{-}C_5H_5)_3(\eta^5\text{-}C_5H_4CONH(CH_2)_{11}SH]$,† **2**, in homoleptic Brust–Schiffrin-type undecanethiolate-AuNPs[12] was achieved in CH_2Cl_2 by mixing undecanethiolate-AuNPs[12] with **2** (one equiv. **2** per coordinated undecanethiol) at room temperature (RT) for 3 days (Scheme 1). The iron-cluster-derivatized AuNPs, **3**, were purified, after removing the solvent under vacuum, by washing the solid residue of **3** with methanol, then with acetone, which allowed the complete separation of **2** and non-functional thiols. The ^1H NMR analysis showed that the proportion of cluster-functionalized thiolate ligand coordinated to the AuNPs **3** was 7%. Elemental analysis (S: 4.10%; Au: 64.73%) corresponds to a Au/S atomic ratio of 2.6, and TEM showed the low dispersity and the average diameter of the Au cores of 2.10 ± 0.5 nm. Combining these two data gives an average number of Au atoms per core of 285 and a number of thiolate ligands $m = 110$, which corresponds to an average of 8 iron-cluster-functionalized thiolates per AuNP, *i.e.* each AuNP contains in average 285 Au (core) and 32 Fe atoms (periphery).

In the second method, we used the direct Brust–Schiffrin-type synthesis[12] by mixing equal amounts of undecanethiol and **2** in toluene with an aqueous solution of $HAuCl_4$ to which $NaBH_4$ was slowly added while stirring (Scheme 1). After 3 h of reaction at RT and the usual work-up procedure,[12] the ^1H NMR spectrum showed that, in the AuNPs obtained (**4**), the $C_{12}H_{25}S/Fe_4$-cluster-thiolate ratio was 52/48, and elemental analysis (S: 3.38%, Au: 45.55%) indicated an atomic ratio Au/S = 2.2. The AuNPs **3** and **4** are air-stable dark-green powders. TEM of **4** (Fig. 1) provided an average diameter of 1.6 ± 0.4 nm corresponding to 101 Au atom per AuNP and 58 thiolate ligands including 28 Fe_4-cluster-functionalized thiolate ligands per AuNP.

The cyclovoltammogram (CV) of **1** was reported to show two reversible monoelectronic oxidation waves and one reversible monoelectronic reduction wave.[9] The CVs of **3** and **4** (Fig. 2) in CH_2Cl_2 on Pt with 0.1 M $n\text{-}Bu_4NPF_6$ resemble that of the monomeric cluster **1**, except that they additionally show adsorption due to the large size of these nanostructures. This analogy is due to the fact that the clusters are sufficiently remote from one another to render the electrostatic factor almost nil. Therefore, all the clusters of **3** or **4** are active at about the same potential.[14,15] For instance, the redox change $Fe_4 \rightarrow Fe_4^+$ appears in a single reversible wave (the wave $Fe_4^0 \rightarrow Fe_4^-$ also is reversible, whereas the wave $Fe_4^+ \rightarrow Fe_4^{2+}$ is only partly chemically reversible with $i_a/i_c < 1$, see Fig. 1). Adsorption is also well visible upon scanning the first oxidation wave. The monoelectronic oxidation wave **1/1**$^+$ is located near 0 V *vs.* ferrocene, whereas the two other CV waves are found at remote positive and negative potentials. These large assemblies also provide facile adsorption onto electrodes for the fabrication of electrodes derivatized with **3** or **4** ($E_{pa} - E_{pc} = 0$ mV) by simple dipping and multiple cycling around the potential of Fe_4/Fe_4^+, whereas for instance the monocluster-derived alkylthiol **2** does not provide a clean modified electrode.

Institut des Sciences Moléculaires, UMR CNRS N°5255, Université Bordeaux I, 33405, Talence Cedex, France. E-mail: d.astruc@ism.u-bordeaux1.fr; Fax: +33 540 00 66 46; Tel: +33 540 00 62 71

† Electronic supplementary information (ESI) available: Experimental procedures for the syntheses of **2**, **3** and **4** from **1**, and titration graph of $H_2PO_4^-$. See DOI: 10.1039/b708466h

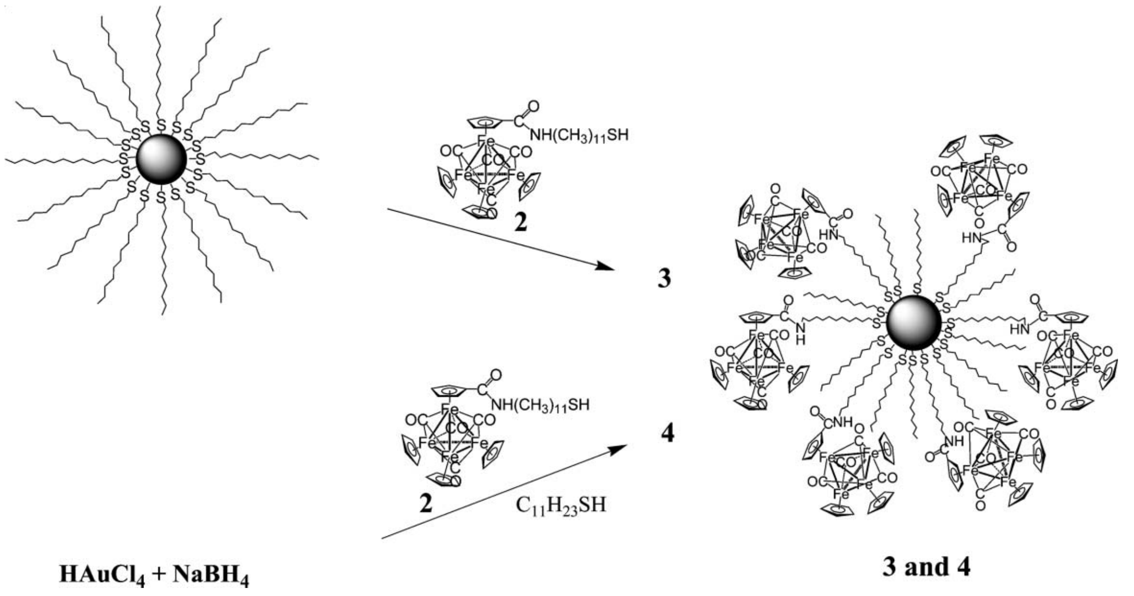

Scheme 1

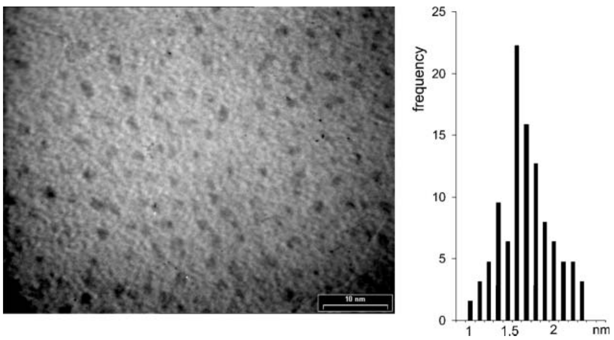

Fig. 1 TEM photograph and size distribution histogram of AuNP **4**, synthesized by the direct method.

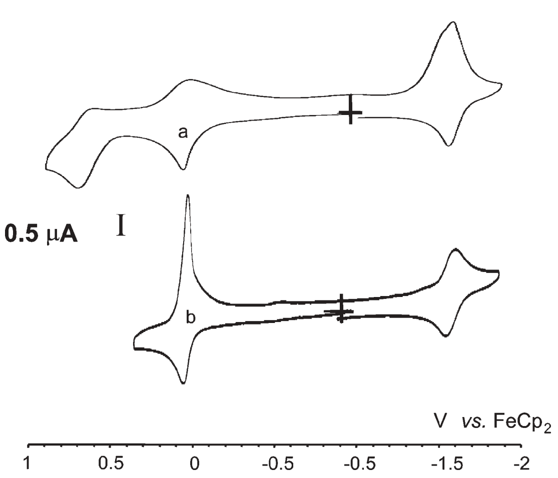

Fig. 2 CV of the Fe_4 cluster-AuNPs **4** (CH_2Cl_2, $[Bu_4N][PF_6]$, 0.1 M; internal reference: $[FeCp_2^*]$; scan rate: 0.1 V s^{-1}); (a) scan of the three waves (top), showing the redox activity of the species resulting from the decomposition of the dicationic clusters (shoulder, top right); (b) scan of only two waves (bottom).

Recognition of oxo-anions by the exo-receptors **3** and **4** was carried out by adding their $N(n\text{-}Bu)_4^+$ salt into the electrochemical cells containing a CH_2Cl_2 solution of the exo-receptor at a Pt anode and was efficient, the oxo-anions $H_2PO_4^-$ and ATP^{2-} disclosing recognition features that are very different from each other and different from those obtained with dendritic ferrocenyl exo-receptors.[3,13]

Addition of $[H_2PO_4]$ $[N(n\text{-}Bu)_4]$ to **4** gives a new CV wave at a potential 60 mV less positive than that of the initial wave whose intensity concomitantly decreases (Fig. 3, left). The replacement of the initial wave by the new wave is much more readily observed and monitored with **4** than with dendrimers whose tethers are terminated with **1**,[10] which allows easier sensing. In the Echegoyen–Kaifer model,[16] this corresponds to a strong-interaction case leading to the ratio of apparent association constants K_+/K_0 = 11 ± 2. There is no cathodic shift of the oxidation wave, which indicates that interaction of $H_2PO_4^-$ with the neutral form is weak. On the other hand, the oxidized form of **4** strongly interacts with $H_2PO_4^-$. The oxo-anion brings electron density onto the cationic Fe_4^+ cluster frame through hydrogen bonding. This makes its oxidation easier, thus occurring at less positive potential than in its absence. This difference of interactive structure between the cationic and neutral cluster forms in **4** is responsible for the large $E_{pa} - E_{pc}$ value at the end of the titration. This phenomenon was not observed to such a large extent in the titration previously using amidoferrocenyl dendrimers.[10] The titration graphs yields a number of $[H_2PO_4]$ $[N(n\text{-}Bu)_4]$ per amido-Fe_4 cluster unit at the equivalent point of 1.3, in accord with a one-to-one interaction. The AuNPs are best suitable for the recognition of $[H_2PO_4]$ $[N(n\text{-}Bu)_4]$, because the strong interaction between the oxidized form of **3** or **4** and $H_2PO_4^-$ brings about a clear-cut phenomenon. We believe that this is due to the large number of amidocluster units in the AuNP defining narrow channels that afford a tight interaction between the amido groups and the small oxo-anion.

Addition of adenosine-5′-triphosphate, ATP^{2-} as its $N(n\text{-}Bu)_4^+$ salt into the electrochemical cell containing the CH_2Cl_2 solution of **4** provokes the appearance of a new CV wave at a potential

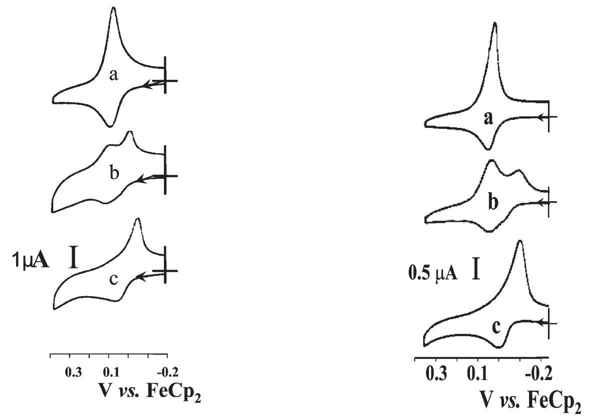

Fig. 3 Titration of [(n-Bu)$_4$N][H$_2$PO$_4$] (left) and of [(n-Bu)$_4$N]$_2$ [ATP] (right) by **4** in CH$_2$Cl$_2$. CVs: supporting electrolyte, 0.1 M [(n-Bu)$_4$N] [PF$_6$]; reference electrode, Ag; auxiliary and working electrode Pt, internal reference, FeCp$_2$*; scan rate, 0.2 V cm^{-1}. (a) **4** alone; (b) in the course of titration, new wave for **4**, $E_{1/2\text{initial}} - E_{1/2\text{new}} = 0.060$ V for H$_2$PO$_4^-$; and 0.095 V for ATP^{2-}; (c) with excess of salt of anion.

150 mV less positive than the initial wave. This new wave is much better separated from the initial wave, however, in the case of ATP^{2-} than with H$_2$PO$_4^-$ (Fig. 3, right). The K_+/K_0 ratio for ATP^{2-} is 43 ± 8, *i.e.* much larger than with H$_2$PO$_4^-$. This means that the interaction between the cationic form of the cluster in **4** and this dianion is stronger than with the monoanion H$_2$PO$_4^-$, probably due to the charge difference between these two anions. Thus, recognition of ATP^{2-} is easier than that of H$_2$PO$_4^-$. This is in sharp contrast with all the previous studies with ferrocenyl dendrimers[13] whereby the recognition of [H$_2$PO$_4$] [N(n-Bu)$_4$] and [ATP] [N(n-Bu)$_4$]$_2$ gave similar results, the recognition of ATP^{2-} being slightly disfavored compared to that of H$_2$PO$_4^-$. The large size difference between H$_2$PO$_4^-$ and ATP^{2-} and the charge difference are responsible for the new observed selectivities that were absent with ferrocenyl-terminated dendrimers and AuNPs. The Fe$_4$-cluster offers a larger frame providing a better possibility of encapsulation by ATP^{2-} than ferrocene and interaction sites with the carbonyl ligands that are susceptible to give rise to additional supramolecular interactions compared to ferrocene.

In addition, a new oxidation wave also appears in the course of titration. This shows that, contrary to what is observed with H$_2$PO$_4^-$, the interaction between the neutral form of the cluster and ATP^{2-} is strong enough to induce a change of oxidation potential. The difference of shifts of potential of the new oxidation and reduction waves confirms that, as expected, the interaction between ATP^{2-} and the cluster is much stronger in the oxidized cluster form (reduction waves) than in the neutral one (oxidation waves).

The titration diagram (Fig. 4) shows an equivalent point close to 0.5 (0.55) equivalent [ATP] [N(n-Bu)$_4$]$_2$ per Fe$_4$-cluster branch due to the double negative charges, which means that each of the two negatively phosphate monoanion units of ATP^{2-} interacts with a Fe$_4$-cluster branch. Other stoichiometries have been reported in such titrations.[6]

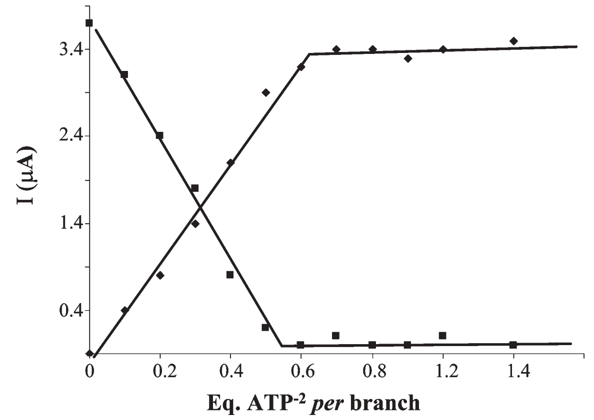

Fig. 4 Titration of ATP^{2-} with AuNP **4** in CH$_2$Cl$_2$. Decrease of the intensity of the initial CV wave (■) and increase of the intensity of the new CV wave (◆) *vs.* the number of the equiv of [n-Bu$_4$N] [ATP] added per cluster branch of **4** (3 × 10^{-5} M).

In conclusion, the first cluster-AuNP assemblies were synthesized using two routes, the direct Brust–Schiffrin synthesis being more efficient than the thiolate ligand-substitution procedure. Redox recognition of oxo-anions is easier than with ferrocenyl dendrimers or AuNPs, and ATP^{2-} provokes a larger CV wave shift than H$_2$PO$_4^-$ contrary to titrations using ferrocenyl-based exoreceptors. These features show the advantage of the use of both AuNPs and the large cluster **1** for sensing over dendritic and ferrocenyl-based exoreceptors.

Notes and references

1 P. D. Beer, *Angew. Chem., Int. Ed.*, 2001, **40**, 486; J. H. R. Tucker and S. R. Collison, *Chem. Soc. Rev.*, 2002, **31**, 147; P. D. Beer and E. J. Hayes, *Coord. Chem. Rev.*, 2003, **240**, 167.

2 W. W. H. Wong, D. Curiel, S.-W. Lai, M. G. B. Drew and P. D. Beer, *Dalton Trans.*, 2005, 774; P. D. Beer and S. R. Bayly, *Top. Curr. Chem.*, 2005, **255**, 125; M. D. Lankshear, A. R. Cowley and P. D. Beer, *Chem. Commun.*, 2006, 612.

3 D. Astruc, M.-C. Daniel and J. Ruiz Aranzaes, *Chem. Commun.*, 2004, 2637.

4 C. M. Casado, I. Cuadrado, B. Alonso, M. Moran and J. Losada, *J. Electroanal. Chem.*, 1999, **463**, 87.

5 C. M. Casado, I. Cuadrado, M. Morán, B. Alonso, B. García, B. González and J. Losada, *Coord. Chem. Rev.*, 1999, **185–186**, 53.

6 O. Reynes, J.-C. Moutet, J. Pecaut, G. Royal and E. Saint-Aman, *New J. Chem.*, 2002, **26**, 9; O. Reynes, C. Bucher, J.-C. Moutet, G. Royal, E. Saint-Aman and E. M. Ungureanu, *J. Electroanal. Chem.*, 2005, **2**, 580.

7 I. Cuadrado, M. Morán, C. M. Casado, B. Alonso and J. Losada, *Coord. Chem. Rev.*, 1999, **193–195**, 395.

8 C. Valério, J.-L. Fillaut, J. Ruiz, J. Guittard, J.-C. Blais and D. Astruc, *J. Am. Chem. Soc.*, 1997, **119**, 2588; C. Valério, E. Alonso, J. Ruiz, J.-C. Blais and D. Astruc, *Angew. Chem., Int. Ed.*, 1999, **38**, 1747.

9 J. A. Ferguson and T. J. Meyer, *J. Am. Chem. Soc.*, 1972, **94**, 3409; J. Ruiz, F. Ogliaro, J.-Y. Saillard, J.-F. Halet, F. Varret and D. Astruc, *J. Am. Chem. Soc.*, 1998, **120**, 1163.

10 J. Ruiz Aranzaes, C. Belin and D. Astruc, *Angew. Chem., Int. Ed.*, 2006, **45**, 132.

11 (*a*) M.-C. Daniel and D. Astruc, *Chem. Rev.*, 2004, **104**, 293; (*b*) *Nanoparticles*, ed. G. Schmid, Wiley-VCH, Weinheim, 2004.

12 M. Brust, M. Walker, D. Bethell, D. J. Schiffrin and R. Whyman, *J. Chem. Soc., Chem. Commun.*, 1994, 801; M. Brust and C. J. Kiely, *Colloids Surf., A*, 2002, **202**, 175; C. A. Waters, A. J. Mills, K. A. Johnson and D. J. Schiffrin, *Chem. Commun.*, 2003, 540.

13 A. Labande, J. Ruiz and D. Astruc, *J. Am. Chem. Soc.*, 2002, **124**, 1782; M.-C. Daniel, J. Ruiz, S. Nlate, J.-C. Blais and D. Astruc, *J. Am. Chem. Soc.*, 2003, **125**, 2617.

14 J. B. Flanagan, S. Margel, A. J. Bard and F. C. Anson, *J. Am. Chem. Soc.*, 1978, **100**, 4248.

15 N. Connelly and W. E. Geiger, *Chem. Rev.*, 1996, **96**, 877.

16 S. R. Miller, D. A. Gustowski, Z.-H. Chen, G. W. Gokel, L. Echegoyen and A. E. Kaifer, *Anal. Chem.*, 1988, **60**, 2021.